Spectral characterization of laser-accelerated protons with CR-39 nuclear track detector

M. Seimetz,[1, a)] P. Bellido,[1] P. García,[1] P. Mur,[1] A. Iborra,[1] A. Soriano,[1] E. Hülber,[2] T. Hülber,[2] J. García López,[3] M.C. Jiménez-Ramos,[3] R. Lera,[4] A. Ruiz-de la Cruz,[4] I. Sánchez,[4] R. Zaffino,[5] L. Roso,[6] and J.M. Benlloch[1]

[1)] *Instituto de Instrumentación para Imagen Molecular (I3M), CSIC - Universidad Politécnica de Valencia - CIEMAT, Camino de Vera s/n, Ed. 8B-N-1a, 46022 Valencia, Spain*

[2)] *Radosys Kft., Vegyész u. 17-27, 1116 Budapest, Hungary*

[3)] *Centro Nacional de Aceleradores (CNA), U. Sevilla - J. Andalucía - CSIC, Avda. Thomas Alva Edison 7, 41092 Sevilla, Spain*

[4)] *Proton Laser Applications S.L. (PLA), Avda. Vilafranca del Penedès 11, 08734 Olèrdola, Spain*

[5)] *Instituto de Microelectrónica de Barcelona (IMB-CNM, CSIC), C/ dels Til.lers Campus UAB, 08193 Cerdanyola del Vallès (Barcelona), Spain*

[6)] *Centro de Láseres Pulsados (CLPU), Calle del Adaja, 37185 Villamayor, Spain*

(Dated: 4 October 2017)

I. INTRODUCTION

The acceleration of protons by highly intense pulses of femtosecond lasers is a field of very active research with many potential applications.[1] The spectral distribution of the protons varies strongly with the experimental conditions and its precise measurement is an essential part of related experiments. The biggest challenge resides in the detection of a large number of particles (of the order 10^8/msr) which are produced almost instantaneously and which energies are typically spread over the entire range up to a certain maximum []. For a quantitative characterization protons of different energies may be separated spatially (in magnetic fields []) or by the time-of-flight technique[2]. In addition, passive detector materials have often been used due to their easy handling and their lack of sensitivity to electromagnetic noise[3]. These comprise radiochromic films which allow for highly resolved analysis of the beam profile[4,5] and CR-39 plates, the latter being especially useful at small particle densities and for a clear separation between protons and ions from electrons and photons.

CR-39 has been applied in different ways for the detection of laser-accelerated protons. Multi-MeV protons can be absorbed in CR-39 stacks, possibly with additional, passive materials in front, in order to obtain their energies from the range and corresponding energy loss[6]. For protons between 0.9 and 2.5 MeV a method based on multiple etching has been proposed recently[7]. However, for practical purposes a single processing cycle (etching and track analysis) of CR-39 plates is preferred, especially for elevated numbers of samples. The main objective of the present work is to measure particle energies directly from the track sizes. Previous studies showed that above 1 MeV approximately the diameters of etched tracks become smaller with increasing proton energy as the ionisation density decreases[8]. The opposite tendency, an increase of track size for higher energies, has been observed below 1 MeV in some publications, indicating a strong dependence on the etching conditions. Lee *et al.*[9] measured a maximum track diameter of 14.3 µm for 0.3 MeV protons after 6 hours etching at 70°C in 6N NaOH. Under the same conditions, similar observations have been made more recently by Baccou *et al.*[10]. A more abundant calibration was presented by Malinowska and coworkers[11] for a 6.25N NaOH bath at 70°C, finding a clear relation between the maximum track size and the etching time (4-20 hours).

Inspired mainly by this latter publication we have sought for a method of extracting quantitative proton spectra directly from the distribution of track sizes on single CR-39 plates. This requires a one-to-one relation between track diameters and proton energies. In order to establish this relation we have irradiated CR-39 samples with monoenergetic protons from a tandem accelerator (section II). For a practical use it is necessary to guarantee a limited processing time after irradiation of the plates, including etching, scanning, and image processing; particle spectra should be extracted within a few hours after a laser-acceleration experiment. We have evaluated different etching conditions and image analysis procedures to find a suitable procedure (section III). Finally, we have used this procedure to analyse samples of laser-accelerated protons (section IV). Our work focusses on proton energies between 0.2 and 5.5 MeV corresponding to the expected cinematic range at a few TW laser power.

II. SAMPLE IRRADIATION WITH MONOENERGETIC PROTON BEAMS

All experiments of the present study have been carried out with CR-39 plates of 10×10 mm^2 size and 0.9 mm thickness (Radosys, Hungary). An etching bath con-

[a)] Corresponding author. Email: mseimetz@i3m.upv.es

tainer with remote controlled temperature has been provided by the same company. Calibration data with monoenergetic proton beams have been taken at the 3 MV tandem accelerator of the Spanish National Accelerator Centre (CNA, Seville). The beam energy can be freely adjusted between 0.7 and 5.5 MeV, with a precision of a few keV. To extend the proton energy range below 0.7 MeV mylar foils with a total thickness of 10 µm have been placed in front of the CR-39 plates. The resulting energies and their corresponding uncertainties in this interval lie between 100 ± 49 keV and 508 ± 33 keV as calculated with SRIM[12]. A total of 19 different beam energies have been selected in the overall interval (0.1 - 5.5 MeV) and several samples have been irradiated for each one.

In order to avoid major numbers of overlapping tracks due to saturation the particle flux has been controlled as follows. The minimum, continuous beam current of the tandem accelerator is about 1 pA or 6×10^6 protons per second which are distributed over an area of 1 cm^2 defined by a rhombic collimator. The beam profile was not uniform. A beam kicker between the proton source and the tandem, coupled to a pulse generator, has been used to produce bunches of 0.1-10 ms length at 1 Hz, reducing the mean particle number by a factor 10^2-10^4. A beam monitor based on a plastic scintillator with PMT readout on a fast oscilloscope[13] allowed for direct verification of the proton flux in the target spot. This control measurement was carried out after beam optimisation at each energy setting, before moving the samples into the beam position. Thus, every CR-39 plate was hit by a total of 10^3-10^4 protons within a few seconds irradiation time, resulting in sufficient numbers of non-overlapping tracks to allow for statistically significant analysis of typical diameters corresponding to each beam energy.

The nuclear track detectors have been etched with 6.25N NaOH at 90°C with varying etching times (2-6 hours). One control series has been etched at 70°C during 4 hours.

III. SCANNING PROCEDURES AND IMAGE PROCESSING

The measurement of the track size and particle numbers requires scanning of major parts of the irradiated surfaces and results in elevated numbers of images for each single CR-39 plate. This has been achieved with a scanning microscope (Radosys PT10). The pixel size of 0.6 µm is far below the diameter of typical proton tracks. We have developped a software code based on ROOT[14] for the identification and size measurement of tracks on these images over a wide range of diameters. It comprises an edge detection algorithm for the search of track borders. A Hough transform is used to identify circular patterns (track ellipticity is not considered as we work at normal particle incidence in all our experiments). It is iterated over a predefined range of diameters to search for the best match.

Representative subsets of images have been processed for each proton energy (examples are presented in Figure 1) and the corresponding distributions of measured track diameters have been represented in histograms (Figure 2). They typically show clear peaks around a central value. Several factors contribute to the finite width of these peaks, the most important one being true differences in the track sizes even of "monoenergetic" samples. Between 0.2 and 0.5 MeV these variations mainly stem from the inherent differences of protons energies due to straggling in the absorber foils. Some particles may be scattered on the collimator edges and lose part of their energy. No clear tracks of equal size have been identified at 0.1 keV, in agreement with former publications []. For each setting, the mean value and standard deviation around the peak are interpreted as nominal track size and its corresponding experimental error, respectively.

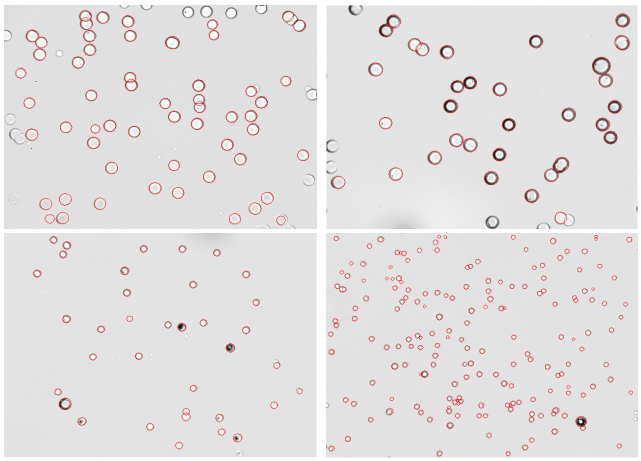

FIG. 1. (Color online) Proton tracks of calibration samples for 0.7 MeV, 1.0 MeV, 2.35 MeV, and 4.5 MeV beam energy, etched at 90°C during 4 hours.

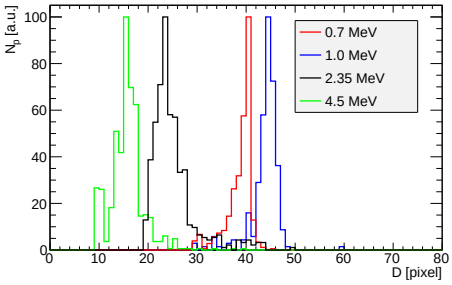

FIG. 2. (Color online) Track diameter distributions of calibration samples. For illustration, the counts have been normalised to the same maximum height.

For proton energies, E_p, increasing from 0.2 to 1 MeV approximately (interval I_1), the mean track diameters, D_t, increase rapidly. Beyond a maximum around 1 MeV, which position slightly varies according to the etching

conditions, and continuing through the entire investigated range (interval I_2), protons of higher energies produce smaller tracks (Figure 3). These observations are qualitatively consistent with previous publications, especially by Malinowska *et al.*[11] (the calibrated range by Sinenian and coworkers[8] started from 1 MeV, comprising only the decreasing interval). The principal, quantitative difference resides in the large pit sizes due to the high etching temperature of 90°C. After 4 hours track diameters up to 26 µm are reached; at 70°C, about 20 hours are necessary to obtain similar values[11]. This implies a strong gradient, $dE_p/dD_t \simeq 2.5$ µm/(100 keV), in I_1 allowing for a clear separation of different proton energies with 0.6 µm wide image pixels. The gradient is much smaller after 2 hours etching, with a maximum of 16 µm diameter. After 6 hours, in turn, the track identification does not further improve, and the number of overlapping tracks increases. We therefore have selected the 4 hours sample as our reference for the remainder of this study.

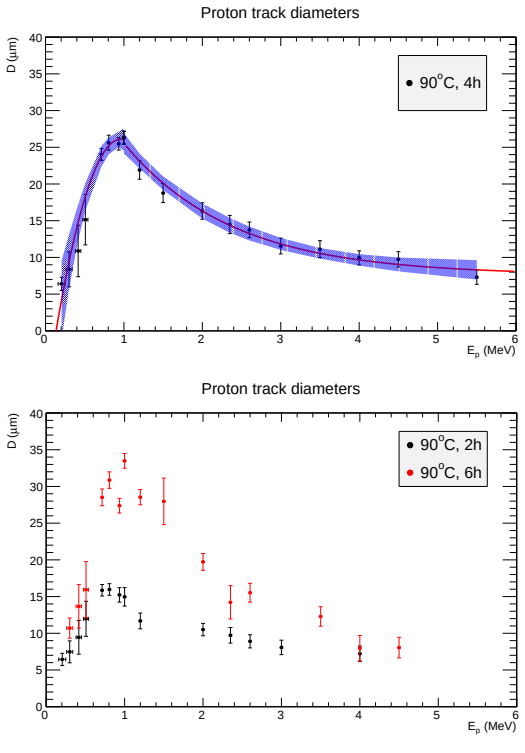

FIG. 3. (Color online) Measured track diameters as a function of proton energy. a) 4 hours etching at 90°C. b) 2 hours and 6 hours at 90°C.

The data trends of the two intervals have been approximated by simple analytical functions,

$$D_t = a_0 + a_1 E_p + a_2 E_p^2 \qquad (1)$$

for I_1 ($E_p \leq 1$ MeV) and

$$D_t = b_0 + b_1 e^{-b_2 E_p} \qquad (2)$$

for I_2 ($E_p \geq 1$ MeV). The data point at 1.0 MeV forms part of both fitted samples. The results for the 4 hours data set are shown in Figure 3 together with the 95% confidence intervals; the fit parameters are summarized in Table I. Eq. (1) can be inverted to obtain proton energies from the measured track diameters,

$$E_p(D_t) = \sqrt{\frac{D_t - a_0}{a_2} + \left(\frac{a_1}{2a_2}\right)^2} - \frac{a_1}{2a_2}\,. \qquad (3)$$

Obviously, this holds only as long as all protons incident on the CR-39 plates are below 1 MeV. Despite this limitation the proposed technique can provide precise particle spectra as will be shown in the following section.

a_0	-9.24 ± 4.61	b_0	7.61 ± 1.12
a_1	73.63 ± 13.69	b_1	36.92 ± 4.19
a_2	-38.35 ± 9.53	b_2	0.722 ± 0.134

TABLE I. Fitted parameters for the sample of Figure 3(a).

IV. APPLICATION TO LASER-ACCELERATED PROTONS

We have used the CR-39 plates of 1 cm^2 size for the spectral characterisation of protons from laser-plasma interactions. These experiments have been carried out on a 3 TW, table-top Ti:Sapphire laser with up to 165 mJ focussed energy on the laser target in 55 fs pulses (details of the setup have been reported in[15]). Consider first an example at low laser intensity (93 mJ on a 7 µm thick aluminium target foil). Fig. 4(a) shows an image of a CR-39 plate placed 230 cm behind the target and directly exposed to the particle flux from a single laser shot. The etching conditions and image processing are as described in section III, resulting in a distribution of track diameters (Fig. 4(b)). For the smallest track sizes relatively large differences between neighbouring bins can be seen. This results from finite binning effects of the automatic track recognition algorithm. The main part of the distribution is smooth. The track diameters are converted into proton energies by eq. (3) as shown in Fig. 5. The binning of this spectral distribution corresponds to the pixel size of the initial image. As the conversion to the energy scale is nonlinear the final bins are not of equal width as is indicated by the horizontal error bars. The vertical error bars correspond to the square root of counts of each bin in Fig. 4(b). To obtain absolute particle numbers per solid angle a scale factor is applied taking into account the total area of analysed, microscopic images and the target distance. The spectral shape can be approximated by an exponential decrease up to a sharp maximum energy, $E_{\max}$, which is typical of laser-accelerated protons (in TNSA). The number of protons, N_p, of energy E_p may be represented analytically by

$$N_p = \frac{N_0}{E_p} \cdot e^{-E_p/E_0} / (1 + e^{(E_p - E_{\max})/\Delta E})\,. \qquad (4)$$

Here, E_0 is interpreted as the mean temperature. The parameter ΔE has been introduced in the term in parantheses to reproduce the finite width of the fall-off. In this case, $E_0 = (868.4 \pm 163.4)$ keV, $E_{\max} = (781.8 \pm 12.3)$ keV, and $\Delta E = (22.0 \pm 8.7)$ keV have been obtained from a fit to the data.

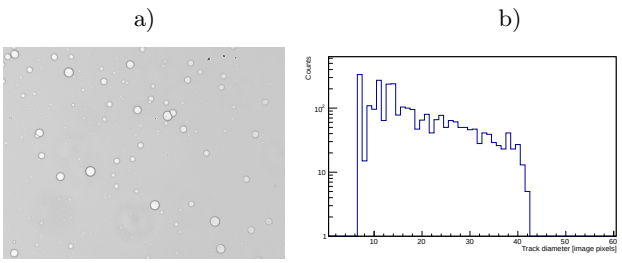

FIG. 4. a) Microscopic image of a CR-39 plate without absorber foil, exposed to a single laser shot at low intensity. b) Distribution of track diameters obtained from a series of images of the same plate.

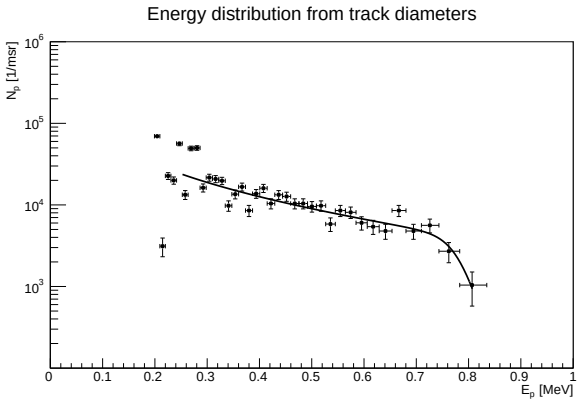

FIG. 5. Proton spectra extracted from the CR-39 plate of Fig. 4.

At low laser intensity like the measurement described above the proton energies were found to be well within the turning point of the calibration curve (below 1 MeV). For tests at higher laser energy (165 mJ on target) our setup has been slightly modified. For each laser shot, four CR-39 plates have been arranged around a central hole (Fig. 6) to allow for simultaneous observation of protons from the same shot on a time-of-flight detector[13]. The opening angle of the proton beam (typically around 10°) is much larger than the lateral displacement of the plates ($\sim 1°$), thus we expect very similar particle spectra from both kinds of measurement. The target distance was 100 cm. In addition, the CR-39 plates have been covered with aluminium foils of different thicknesses, for two purposes. On the one hand, to absorb the dominant, low-energetic part of the continuous spectral distributions and thus avoid saturation due to overlapping tracks. And on the other hand, to reduce the energy of the remaining particles and shift them to the calibrated range below 1 MeV. The corresponding energy loss has been calculated with SIMNRA[16]. For a given absorber thickness, $d_{\rm abs}$, incident protons must possess a minimum kinetic energy, $E_{\min}$, to exceed the detection limit on the subsequent CR-39 plate (200 keV) and produce clear tracks (Table II). Similarly, the initial energy of the protons must not exceed a maximum, $E_{\max}$, to make sure that they fall inside the calibrated range below 1 MeV.

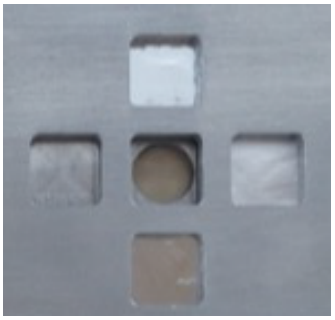

FIG. 6. (Color online) Support structure for four individual CR-39 plates, each one covered with aluminium foils of different thicknesses. Part of the protons pass through the central hole and hit the time-of-flight detector.

$d_{\rm abs}$/µm	$E_{\min}$/keV	$E_{\max}$/keV
4	525	1200
7	750	1300
10	875	1400
12.5	990	1500
18	1225	1700
25	1500	1925
35	1850	2200
43	2100	2400
50	2275	2600

TABLE II. Minimum and maximum incident proton energies on aluminium foils of thickness $d_{\rm abs}$ corresponding to the calibrated range of detected energies on CR-39 plates.

As a second example, consider CR-39 plates obtained from a single laser shot on a 2 µm thick mylar target foil ("target 2"). Individual tracks can clearly be distinguished when 7 µm or 10 µm thick absorbers are used (Fig. 7). With thinner aluminium foils the tracks overlap and their sizes cannot be resolved. Following the procedure described in section III the distribution of track diameters is obtained for a representative selection of microscopic images of each plate. The track diameters are converted into proton energies incident on the CR-39 plates by eq. (3). Subsequently, the initial particle energy (from the laser-plasma interaction) is calculated correcting for the energy loss in the absorber.

In Fig. 7, the data points from a CR-39 plate covered with a 7 µm thick absorber start around 750 keV as stated in Table II. They correspond to proton numbers of the order 10^5/msr up to 0.93 MeV where a sudden decrease is observed. The same analysis has been performed for the plate covered with a 10 µm thick absorber. Here,

the overall range of detected particle energies is smaller (starting from 875 keV) and the particle numbers per bin decrease rapidly at 1.02 MeV. Both spectra are compared to the particle energy distribution which has been obtained for the same laser shot using the time-of-flight detector (continuous line in Fig. 7; for details of the analysis and normalization procedure see[15]). The three independent measurements give similar values for the maximum proton energy within a full range of (0.98 ± 0.05) MeV.

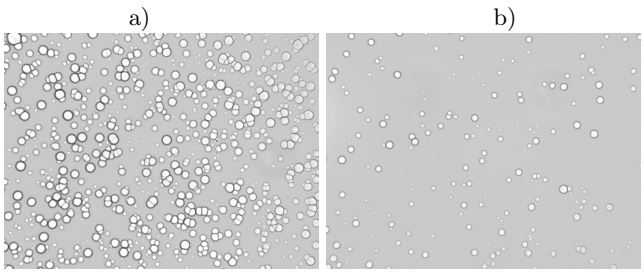

FIG. 7. Microscopic images of CR-39 plates after a single laser shot (target 2), covered with (a) 7 µm and (b) 10 µm of aluminium, respectively.

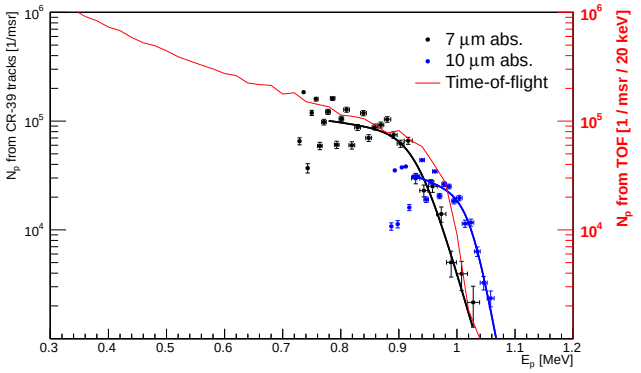

FIG. 8. (Color online) Comparison of proton spectra extracted from CR-39 plates covered with 7 µm and 10 µm aluminium foils, respectively. The thin curve shows the spectra of the same shot reconstructed from the time-of-flight detector.

In the previous example, the highest particle energies were still close to the range allowing for a one-to-one correspondence between track diameters. We have studied the applicability of our method also for the case of significantly higher proton energies. This is demonstrated with a single laser shot of 165 mJ on a 0.65 µm thin aluminium membrane produced with MEMS techniques from a silicon wafer. Four CR-39 plates have been arranged as described above, but covered with thicker absorber foils (18-43 µm of aluminium). With 18 µm and 25 µm covers the track density is too high for a spectral analysis (Fig. 9(a)). With a 35 µm absorber, to the contrary, individual tracks with a wide range of diameters can be observed (Fig. 9(b)). Following the procedure described previously the spectra of Fig. 10 has been reconstructed. Here again, the maximum proton energy (2.08 MeV) compares well with the result of the time-of-flight measurement of the same laser shot. In this case, only the region close to the end point of the spectral distribution can be investigated by our method which, however, allows for an independent check of the results obtained with a different type of detector.

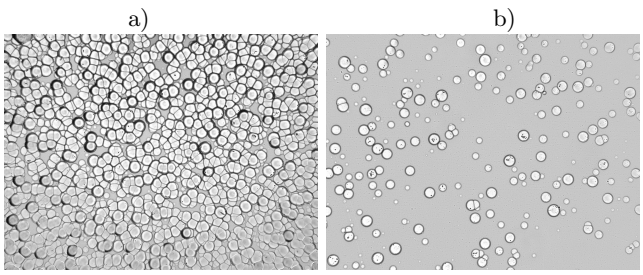

FIG. 9. Microscopic images of CR-39 plates exposed to a single laser shot (target 3), covered with (a) 25 µm and (b) 35 µm of aluminium, respectively.

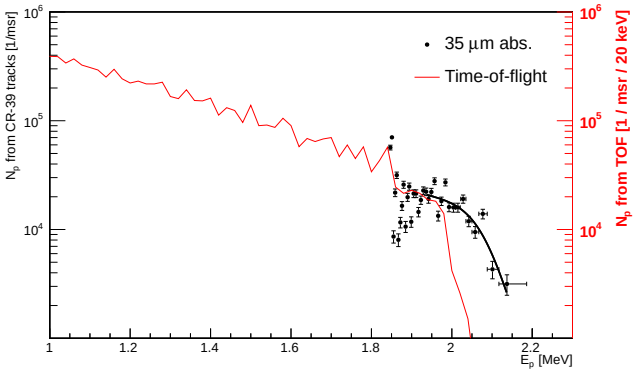

FIG. 10. (Color online) Proton spectra extracted from CR-39 plates covered with a 35 µm aluminium foil (target 3). The thin line shows the spectra of the same shot reconstructed from the time-of-flight detector.

V. CONCLUSIONS

We present a method of determining spectral properties of laser-accelerated protons using CR-39 track detector. Proton energies between 0.2 MeV and 1.0 MeV are directly correlated with the track diameters. Etching at 90°C during 4 hours allows for fully exploiting this equivalence as we have shown in calibration measurements. We have applied our method to laser-accelerated protons in different working regimes. At low laser intensities where particle energies do not exceed 1 MeV precise spectra can be extracted from one irradiated CR-39 plate and after a single etching and image analysis procedure.

At higher intensities and correspondingly elevated particle energies and track densities, several CR-39 plates can be covered with absorber foils of different thicknesses to shift the detected part of the spectra to the calibrated range. This allows for a precise determination of the maximum proton energies. The information obtained in this way is much more precise than "binary" measurements based on the mere observation of tracks behind absorbers of different thicknesses.

The proposed method may be limited to maximum proton energies below 10 MeV and, correspondingly, moderate laser energies (≤ 1 J) as straggling in the absorbers becomes increasingly important at larger thicknesses. Nevertheless, it may be a useful tool for experiments in a regime accessible for cost-effective, tabletop lasers. Further, it allows for cross-checks of results obtained from alternative detection techniques, a task which is still challenging at high particle intensities in very short pulses.

ACKNOWLEDGMENTS

The authors appreciate the collaboration of the CNA accelerator operators. This project has been funded by the Spanish Ministry for Economy and Competitiveness within the Retos-Colaboración 2015 initiative, ref. RTC-2015-3278-1. P. Mur has been awarded a Garantía Juvenil grant.

[1] H. Daido, M. Nishiuchi, and A. S. Pirozhkov, "Review of laser-driven ion sources and their applications," Reports on Progress in Physics **75**, 056401 (2012).

[2] A. Yogo, H. Daido, A. Fukumi, Z. Li, K. Ogura, A. Sagisaka, A. S. Pirozhkov, S. Nakamura, Y. Iwashita, T. Shirai, A. Noda, Y. Oishi, T. Nayuki, T. Fujii, K. Nemoto, I. Woo Choi, J. Hee Sung, D.-K. Ko, J. Lee, M. Kaneda, and A. Itoh, "Laser prepulse dependency of proton-energy distributions in ultraintense laser-foil interactions with an online time-of-flight technique," Physics of Plasmas **14**, 043104 (2007).

[3] P. Bolton, M. Borghesi, C. Brenner, D. Carroll, C. D. Martinis, A. Flacco, V. Floquet, J. Fuchs, P. Gallegos, D. Giove, J. Green, S. Green, B. Jones, D. Kirby, P. McKenna, D. Neely, F. Nuesslin, R. Prasad, S. Reinhardt, M. Roth, U. Schramm, G. Scott, S. Ter-Avetisyan, M. Tolley, G. Turchetti, and J. Wilkens, "Instrumentation for diagnostics and control of laser-accelerated proton (ion) beams," Physica Medica **30**, 255–270 (2014).

[4] F. Nürnberg, M. Schollmeier, E. Brambrink, A. Blažević, D. C. Carroll, K. Flippo, D. C. Gautier, M. Geißel, K. Harres, B. M. Hegelich, O. Lundh, K. Markey, P. McKenna, D. Neely, J. Schreiber, and M. Roth, "Radiochromic film imaging spectroscopy of laser-accelerated proton beams," Review of Scientific Instruments **80**, 033301 (2009).

[5] C. Scullion, D. Doria, L. Romagnani, H. Ahmed, A. Alejo, O. Ettlinger, R. Gray, J. Green, G. Hicks, D. Jung, K. Naughton, H. Padda, K. Poder, G. Scott, D. Symes, S. Kar, P. McKenna, Z. Najmudin, D. Neely, M. Zepf, and M. Borghesi, "Angularly resolved characterization of ion beams from laser-ultrathin foil interactions," Journal of Instrumentation **11**, C09020 (2016).

[6] A. Zigler, S. Eisenman, M. Botton, E. Nahum, E. Schleifer, A. Baspaly, I. Pomerantz, F. Abicht, J. Branzel, G. Priebe, S. Steinke, A. Andreev, M. Schnuerer, W. Sandner, D. Gordon, P. Sprangle, and K. W. D. Ledingham, "Enhanced proton acceleration by an ultrashort laser interaction with structured dynamic plasma targets," Phys. Rev. Lett. **110**, 215004 (2013).

[7] F. Bahrami, F. Mianji, R. Faghihi, M. Taheri, and A. Ansarinejad, "Response of cr-39 to 0.9-2.5 mev protons for koh and naoh etching solutions," Nuclear Instruments and Methods in Physics Research Section A: Accelerators, Spectrometers, Detectors and Associated Equipment **813**, 96 – 101 (2016).

[8] N. Sinenian, M. J. Rosenberg, M. Manuel, S. C. McDuffee, D. T. Casey, A. B. Zylstra, H. G. Rinderknecht, M. G. Johnson, F. H. Sguin, J. A. Frenje, C. K. Li, and R. D. Petrasso, "The response of cr-39 nuclear track detector to 1-9 mev protons," Review of Scientific Instruments **82**, 103303 (2011).

[9] J. Lee, J. Jo, S. Park, K. Lee, Y. Lee, K.-H. Yea, Y. Cha, and Y. Jeong, "Study on the tracks in a nuclear track detector (cr39) for detection of laser-induced charged particles," J. Korean Phys. Soc. **51**, 426–430 (2007).

[10] C. Baccou, V. Yahia, S. Depierreux, C. Neuville, C. Goyon, F. Consoli, R. D. Angelis, J. E. Ducret, G. Boutoux, J. Rafelski, and C. Labaune, "Cr-39 track detector calibration for h, he, and c ions from 0.1-0.5 mev up to 5 mev for laser-induced nuclear fusion product identification," Review of Scientific Instruments **86**, 083307 (2015).

[11] A. Malinowska, A. Szydłowski, M. Jaskóła, A. Korman, B. Sartowska, T. Kuehn, and M. Kuk, "Investigations of protons passing through the cr-39/pm-355 type of solid state nuclear track detectors," Review of Scientific Instruments **84**, 073511 (2013).

[12] J. Ziegler and J. Biersack, "Srim - the stopping range of ions in solids," Pergamon (1985).

[13] M. Seimetz, P. Bellido, A. Soriano, J. G. López, M. C. Jiménez-Ramos, B. Fernández, P. Conde, E. Crespo, A. J. González, L. Hernández, A. Iborra, L. Moliner, J. P. Rigla, M. J. Rodríguez-Álvarez, F. Sánchez, S. Sánchez, L. F. Vidal, and J. M. Benlloch, "Calibration and performance tests of detectors for laser-accelerated protons," IEEE Transactions on Nuclear Science **62**, 3216–3224 (2015).

[14] R. Brun and F. Rademakers, "Root - an object oriented data analysis framework," Nuclear Instruments and Methods in Physics Research Section A: Accelerators, Spectrometers, Detectors and Associated Equipment **389**, 81 – 86 (1997).

[15] P. Bellido, R. Lera, M. Seimetz, A. R. de la Cruz, S. Torres-Peirò, M. Galán, P. Mur, I. Sánchez, R. Zaffino, L. Vidal, A. Soriano, S. Sánchez, F. Sánchez, M. Rodríguez-Álvarez, J. Rigla, L. Moliner, A. Iborra, L. Hernández, D. Grau-Ruiz, A. González, J. García-Garrigos, E. Díaz-Caballero, P. Conde, A. Aguilar, L. Roso, and J. Benlloch, "Characterization of protons accelerated from a 3 tw table-top laser system," Journal of Instrumentation **12**, T05001 (2017).

[16] M. Mayer, "SIMNRA, a simulation program for the analysis of NRA, RBS and ERDA," AIP Conference Proceedings **475**, 541 (1999).